Radiotherapy-Related Neurologic Complications in Patients with Nasopharyngeal Carcinoma: A Multicenter Epidemiologic Study in Southern China

Tong Pan[1], Xiangping Li[2], Bin Zhao[3], Chengguo Zhang[4], Xiaoming Rong[1], Chao Qin[5], Guoqiang Wen[6], Wenjun Wu[7], Hongxuan Wang[1], Kui Lu[7], Haihong Zhou[3], and Ying Peng[1,8]

ABSTRACT

Background: We aim at describing the incidence, potential predisposing factors, and progression of major radiotherapy-related neurologic complications (RRNC) in nasopharyngeal carcinoma (NPC)-endemic regions, especially southern China.

Methods: We performed a multicenter longitudinal retrospective study with clinical follow-ups in 22,302 patients with post-radiotherapy NPC between January 2003 and June 2017 covering three major residential areas. Epidemiology, potential predisposing/protective factors, clinicopathologic progression, and survival conditions of each RRNC were separately recorded and analyzed on the basis of their related clinical, radiologic, and laboratory parameters.

Results: 949 new cases of RRNCs occurred among the 22,302 patients with post-radiotherapy NPC during 101,714 person years' follow-up, which is equal to an incidence density rate of 9.3 new cases per 1000 person year. Radiation-induced cranial nerve palsy showed the highest incidence (2.68%, 597/22,302) with the earliest onset (median latency, 4.45 years) as well. Patients benefited from intensity-modulated radiotherapy (IMRT) over conventional radiotherapy (CRT) in both overall survival (median survival 13.2 years for IMRT vs. 8.3 years for CRT) and RRNC-free survival (except for epilepsy and cranial nerve palsy). Causes of death varied substantially between patients with or without RRNCs.

Conclusions: Our study indicates a non-negligible incidence of RRNC spectrum in southern China in the past ten years. IMRT is one of the most significant protectors against development and progression of RRNCs.

Impact: Our findings support the hypothesis that patients with NPC with preexisting predispositions would receive long-term benefits from IMRT and other dose-related modulations (like hyperfractionation and dose conformation).

Introduction

Nasopharyngeal carcinoma (NPC) remains a highly prevalent malignant disease in parts of southern China (1). Incidence ranges from 15 to 30 per 100,000 person-years in southern China from 2013 to 2018 (2–4), and crude mortality rate ranges from 1.5 to 2.0 per 100,000 people from 1973 to 2015 (4). Given the deep location, complex nasopharyngeal adjacency, and radiation sensitivity, radiotherapy remains the mainstay treatment modality for nonmetastatic disease (5). Over the past few years, photon-based radiotherapy techniques have progressed from conventional two-dimensional radiotherapy (2D-CRT) to 3D conformal radiotherapy, followed by intensity-modulated radiotherapy (IMRT; ref. 3). Although IMRT has provided excellent loco-regional control with relative sparing of organs at risks (OAR), especially brainstem and temporal lobes, late neurotoxicity still occurs with considerable incidence (6, 7). Radiotherapy-related neurologic complications (RRNC) are defined as a spectrum of neurologic complications induced by radiotherapy to head and neck regions. Here are some of the most common RRNCs in current clinical practice: RIBI (radiation-induced brain injury), hypopituitarism, cranial or peripheral nerve palsies (e.g., glossopharyngeal nerve and brachial plexus), radiotherapy-related neuropathic pain, secondary epilepsy, and post-radiotherapy cerebrovascular events (including stroke and carotid artery stenosis). Studies on the epidemiologic characteristics of RRNCs are limited: only a few small-scale retrospective studies trying to figure out the incidence of radiation-induced temporal lobe necrosis (TLN; ref. 8) and brainstem injuries (9). In this 2014 single-center case–control study based on 1,887 patients with post-IMRT NPC, 43 (2.28%) had developed TLN (8). Another study in 2018 (9) revealed that the actuarial incidence rates of MRI-indicated radiotherapy-induced brainstem injury were 2.2% and 2.8% at 3 and 5 years after the completion of radiotherapy.

There have been several studies demonstrating the preventive effect of IMRT on late toxicities of radiation to oropharyngeal and/or nasopharyngeal regions (9–14), but to obtain a more specific, comprehensive, and dynamic view on late-onset neurotoxicity of radiotherapy still requires large-scale population-based cohort studies. Therefore, we collected epidemiologic and follow-up data from seven

[1]Department of Neurology, Sun Yat-Sen Memorial Hospital, Sun Yat-Sen University, Guangzhou, China. [2]Department of Otolaryngology-Head and Neck Surgery, Nanfang Hospital, Southern Medical University, Guangzhou, China. [3]Department of Neurology, Affiliated Hospital, Guangdong Medical College, Zhanjiang, China. [4]Department of Neurology, First People's Hospital of Foshan City, Foshan, China. [5]Department of Neurology, First Affiliated Hospital of Guangxi Medical University, Guangxi, China. [6]Department of Neurology, Hainan General Hospital, Hainan, China. [7]Department of Neurology, the People's Hospital of Zhongshan City, Shanghai, China. [8]Guangdong Provincial Key Laboratory of Malignant Tumor Epigenetics and Gene Regulation, Sun Yat-Sen Memorial Hospital, Sun Yat-Sen University, Guangzhou, China.

Note: Supplementary data for this article are available at Cancer Epidemiology, Biomarkers & Prevention Online (http://cebp.aacrjournals.org/).

T. Pan, X. Li, B. Zhao, and C. Zhang contributed equally to this article.

Current address for T. Pan: First Affiliated Hospital of Sun Yat-Sen University, Guangzhou, Guangdong, China.

Corresponding Author: Ying Peng, Sun Yat-Sen University, No. 33 Yinfeng Road, Haizhu District, Guangzhou 510288, Guangdong, China. Phone: 8602-0340-70667; Fax: 8602-0813-32833; E-mail: pengy2@mail.sysu.edu.cn

Cancer Epidemiol Biomarkers Prev 2022;31:1119–29

doi: 10.1158/1055-9965.EPI-21-0953

individual institutions located in Guangdong province, Guangxi autonomous region and Hainan province, where NPC is among the most common causes of head and neck malignancies (2–4).

Materials and Methods

Patient population

Patients with histopathologic diagnosis of NPC and receiving radiotherapy were enrolled in corresponding residencies between January 2003 and June 2017. Patients with metastatic disease at the time of diagnosis, a prior history of other malignant diseases or previous radiotherapy to the head and neck regions were excluded. Ethics approval for use of patient information without prior consent was granted by all ethics committees of the seven institutions enrolled, including 5 in Guangdong (Sun Yat-Sen Memorial Hospital, Nanfang Hospital, Affiliated Hospital of Guangdong Medical College in Zhanjiang, the First People's Hospital of Foshan City, and the People's Hospital of Zhongshan City), 1 in Guangxi (the First Affiliated Hospital of Guangxi Medical University), and 1 in Hainan (Hainan General Hospital).

We extracted data concerning RIBI, cranial nerve palsy, carotid stenosis, stroke, hypopituitarism, and epilepsy from electronic health record systems of the seven institutions. Baseline demographics (age, gender, residential area, smoking status, alcohol consumption, and comorbidities), tumor characteristics [histologic type, tumor-node-metastasis (TNM), and American Joint Committee of Cancer (AJCC) stage (15, 16)], and treatment plans [method (CRT or IMRT), maximum doses to tumor targets (nasopharyngeal and bilateral neck lymph node regions) and to some OARs in central nervous system (temporal lobes, hypothalamus/pituitary gland, and brainstem), fractionation, reirradiation, and concurrent chemotherapy] were recorded. Severity of comorbidities was based on a modified Charlson comorbidity index (CCI; refs. 17–19; 0 = no comorbidity, 1 = mild to moderate, 2 = severe), which scored and predicted the 10-year survival/mortality risk in patients with multiple major comorbidities. The index was calculated before the initiation of radiotherapy.

All enrolled patients were clinically followed after radiotherapy. We consider one visit to the enrolled hospitals for either a health exam or deterioration as one effective follow-up. It would come to an end till the patient's death from any cause or concurrence of radiotherapy-irrelevant neurologic disorders (like intracranial metastasis and cranial nerve palsies caused by skull base infiltration or surrounding nerve compression due to enlarging primary NPC foci) interfering with clinical observation of the natural history during follow-up, otherwise follow-up would continue till the end of survivor's latest visit. Baselines, antitumor regimen, clinical outcomes were similarly recorded with each follow-up for RRNCs-free individuals. The last date of follow-up in this cohort was March 14, 2018.

Radiation-induced brain injury

Radiation-induced brain injury (RIBI) was defined as radiologic findings of white matter lesion, contrast-enhanced lesion, cyst, and/or necrosis with or without local mass effect (20). Time interval from completion of radiotherapy to first confirmation of RIBI was calculated as latency (21). Apart from the general items mentioned above, cranial MR- or CT-based results were quantified and recorded.

Disease progression was evaluated based on Common Terminology Criteria for Adverse Events (CTCAE) score (22) per visit, concomitant comorbidities over time, and radiologic reviews. Follow-up was ceased till the patient's death from any cause or concurrence of other radiotherapy-irrelevant neurologic disorders interfering with clinical observation of the natural history (23), otherwise it would continue till the end of survivor's latest follow-up.

We stratified RIBI patients' radiologic findings as four components (24, 25): white matter lesion, contrast-enhanced lesion, cyst, and local mass effect. White matter lesion was defined as homogeneous lesion of high signal intensity on T2-weighted but low on T1-weighted image without contrast enhancement. Three levels of lesion were observed: mild = small focus within one lobe, moderate = large and confluent focus within one lobe, severe = large and confluent areas extending outside radiation field. Contrast-enhanced lesion was defined as lesion with or without necrosis on post-contrast T1-weighted images with heterogeneous signal abnormalities on T2-weighted images. Size and appearance of contrast-enhanced lesions were assessed and divided into solid enhanced nodules and rim-enhanced lesions of irregular shape with finger-like projections. Cysts were defined as round or oval well-defined lesions of very high signal intensity on T2-weighted images with a thin or imperceptible wall with or without enhancement. Local mass effect was graded as follows (27): mild = affecting only the sulci, moderate = both the sulci and the ventricle(s) involved, severe = midline shift. These four categories of foci might coexist, appear chronologically, or exist individually (25).

Cranial nerve palsy

Radiation-induced cranial nerve palsy is a subacute-onset complication after months to years from radiotherapy (to head and neck regions) completion with progressive and profound vision and/or hearing loss, eyeball movement disorders, trigeminal neuralgia, facial paralysis, and dysphagia (26). Screening was conducted by physical examinations, and all eligible individuals underwent further investigations (including MRI of nasopharynx and neck, nasopharyngoscopy; biopsy of the nasopharynx or PET-CT was performed if any abnormal lesion was detected) to rule out local recurrence (27). Follow-up items were number(s) of cranial nerve(s) involved, CTCAE score (22), comorbidities during follow-up period, and treatment.

Carotid stenosis

Post-radiotherapy carotid stenosis was diagnosed according to artery ratios (internal carotid artery to common carotid artery) on head and neck CTA/MRA and/or velocities (peak systolic, end diastolic) on bilateral carotid vessel ultrasonography (8). Significant stenosis was defined as stenosis >50% or complete occlusion (8). Ultrasonography including arterial sclerosis, percentage of lumen stenosis, intima-media thickness (IMT), and plaque formation (28) were followed until death, loss to follow-up, or undergoing carotid endarterectomy/stenting procedures (29).

Post-radiotherapy stroke

Confirmation of post-radiotherapy stroke was based on head CT and/or MR (30). Diagnosed patients were followed in symptoms, neurologic signs, head CT/MRIs and newly-onset comorbidities.

Hypopituitarism

Apart from common exclusion criteria, patients with preradiotherapy endocrine abnormalities or tumor extension to parts of hypothalamus–pituitary gland–adrenal axis (HPA) were also excluded (31). Unfortunately, pituitary function and reserve tests were merely conducted on clinical hypopituitarism (32) cases (with major clinical symptoms/signs like extensive debilitation and peripheral edema, with only 38 complete pituitary function assays available), and patterns of endocrine testing varied over time and between institutions.

Symptoms/signs, serum basal hormone and physiotrophic hormone levels, serum electrolytes, and CT/MRI of hypothalamus/pituitary region (if available) were followed subsequently.

Secondary epilepsy

Radiotherapy-related epilepsy could occur both in RIBI and non-RIBI individuals (33). Diagnosis was conducted by more than two experienced neurologists based on medical history (34). Physical examinations, seizure semiology, head CT/MRI, electroencephalogram, and antiepileptic medications were followed.

Statistical analysis

χ^2 test was used for categorical variables and Student *t* test for continuous variables. Where continuous variables were dichotomized into categories, we defined the cut-off point by levels, usually median (22). Ordered categorical variables were compared using Mann–Whitney *U* test.

Specifically, in terms of multivariable survival analysis, based on clinical observations, univariable Cox regression analysis results, and our previous publications (32, 35–36), potential predisposing factors were categorized as: NPC AJCC stage (including I, II, III, IVA, and IV), concurrent chemotherapy (either neoadjuvant or adjuvant chemotherapy), radiotherapy method (IMRT or CRT), maximum radiation doses (D_{max}) to nasopharynx/bilateral neck lymph nodes, fractionation, and reirradiation. Three multivariable Cox regression models with different ranges of adjusting covariates were applied sequentially: (i) Model 1: adjusted for age, gender, and residency; (ii) Model 2 was additionally adjusted for lifestyle-related behaviors (smoking and excessive alcohol consumption) and comorbidities (hypertension, diabetes mellitus, hyperlipidemia, coronary heart disease, and prior stroke); (iii) Model 3 was additionally (compared with Model 2) adjusted for tumor- and treatment-related parameters other than the one being studied. Potential candidates filtered by Models 1 and 2 were further confirmed by Model 3 to check the independence of each risk factor enrolled. Similarly, due to our limited access to detailed radiotherapy-related parameters, only univariable Cox regression analysis was applied to those with complete radiotherapy records reflecting D_{max} to OARs in central nervous system (we focused on brainstem, hypothalamus/pituitary gland, and temporal lobes). Differences in mortality, complication-free rate, and cause of death were detected using log-rank tests via Kaplan–Meier method. Data collection was performed with EpiData version 3.1 (EpiData Institute, Copenhagen, Denmark). Statistical analyses were by SPSS, version 22.0 (IBM Institute), and STATA, version 17.0 (StataCorp). Graphic plotting was conducted by GraphPad Prism, version 7.0 (Graphpad Software) and Microsoft Office Excel, 2021. All statistical tests were two-sided and a P value of <0.05 was considered statistically significant.

Results

Patients and incidence

We identified 35,318 patients with NPC from the records of radiotherapy and otorhinolaryngology department. We excluded 7,348 patients with metastasis on initial diagnosis, history of other malignancies, or prior radiation to head and neck regions. Of the 27,970 remaining patients, 620 did not possess any radiotherapy records, which made it difficult to judge whether they did receive radiotherapy after pathologic confirmation of NPC. 5,048 patients were lost to follow up. Finally, a total of 22,302 consecutive patients with NPC and subsequent radiotherapy were identified. Among them, 949 had been assessed at the neurology department during their follow-up and confirmed as RRNCs (Supplementary Fig. S1). 101,714 person years were followed for the whole cohort. Median age was 53 (22–87) years old. Most of them were males (n = 16,210, 72.7%), nonsmokers (n = 16,915, 75.8%), and with a comorbidity index of 0 (n = 19,748, 88.5%). During a median follow-up of 2.7 years (interquartile range, 1.8–4.9 years), the incidence density rate for RRNC was 9.3/1,000 person year. Area-specific incidences were 4.5% (585/12,770) in Guangdong, 4.2% (278/6,619) in Guangxi, and 3.0% (86/2,913) in Hainan. Radiation-induced cranial nerve palsy was the most frequently occurred and the earliest onset, with an incidence of 2.68% (597/22,302) and a median latency of 4.45 years. 11,480 (51.5%) patients received CRT. Distribution of demographic characteristics was shown in **Table 1**.

We then separately analyzed those six diseases mentioned above. χ^2 test indicated RIBI and cranial nerve palsy were more prevalent in CRT group compared with IMRT (62.8% vs. 54.3%, P = 0.03; 65.5% vs. 53.9%, P = 0.002, respectively). Hypopituitarism occurred more frequently in CRT group, but with marginally significant difference (18.2% vs. 12.5%, P = 0.05).

RIBI

579 (2.60%) individuals developed RIBI. Sixty RIBI patients presented as asymptomatic onset with radiologically confirmed foci. The median latency was 4.70 years.

Categories of onset symptoms/signs were shown in Supplementary Table S1. Notably, cases with similar clinical manifestations irrelevant to intracranial responsible foci (e.g., RIBI patients with concurrent radiation-induced optic nerve injury presented as visual field defect) were excluded to prevent overestimation. 251 (43.4%) presented nonspecific features of intracranial lesions such as mild headache, dizziness, and/or confusion. 51 (8.9%) were severely affected with marked debilitation, high intracranial pressure, generalized epileptic attacks and/or unconsciousness. Frequent symptoms included dizziness (131, 22.6%), headache (126, 21.7%) and pseudobulbar palsy (95, 16.4%). Radiotherapy-related neuropathic pain tended to present more frequently in IMRT (P = 0.001), whereas memory impairment in CRT (P = 0.045). Among the 60 asymptomatic-onset ones, 36 were lost to follow-up. With a median follow-up period of 4.7 years (interquartile range, 3.2–6.7 years) for the remaining 24 cohort, 3 remained asymptomatic (with median follow-up of 4.1 years), and the other 21 exhibited a median latency of 1.0 year from asymptomatic onset to new symptoms debut.

Post-IMRT RIBI tended to appear as unilateral temporal lobe white matter lesion with rim-enhanced pattern; whereas post-CRT RIBI occurred bilaterally and could also be detected in frontal-parietal-occipital lobes and basal ganglia with nodular enhancement (Supplementary Table S2). Evolution of each radiology phenotype could be divided into four groups (17): static, increasing, decreasing or resolved, and fluctuating. Details are shown in Supplementary Table S3. White matter lesions were more likely to remain static (P < 0.001), whereas contrast-enhanced lesions tended to fluctuate (P < 0.001). Local mass effects were predisposed to regression (P = 0.007). Cysts conversely exhibited the tendency to progress (P < 0.001). Next, Evolution tendency of RIBI between CRT and IMRT group was then compared. IMRT was a protective factor against cyst progression or fluctuation (P = 0.008). CRT was related to a higher risk of cyst progression, but the difference was not statistically significant (P = 0.06).

To further explore potential predictors of RIBI, several multivariable Cox regression models adjusted for different ranges of covariables were successively performed (**Table 2**). Notably, here we defined the dose level as "low" if total D_{max}<64 Gy and vice versa, based on

Table 1. Baseline characteristics of enrolled patients.

Characteristics	No. (%) RRNC	No. (%) RRNC-free	*P* value[a]
Total	**949 (100.00)**	**21,353 (100.00)**	**—**
Residential area			<0.001[c]
Guangdong	585 (61.6)	12,185 (57.1)	
Guangxi	278 (29.3)	6,341 (29.7)	
Hainan	86 (9.1)	2,827 (13.2)	
Age at cancer diagnosis (y)			0.38
Mean (95% CI)	50.9 (50.2–51.7)	47.2 (47.1–47.4)	
Standard deviation (SD)	11.6	11.5	
Male	708 (74.6)	15,502 (72.6)	0.18
CCI			0.10
=0	856 (90.2)	18,892 (88.5)	
≥1	93 (9.8)	2,461 (11.5)	
History of hypertension	42 (4.4)	1,291 (6.0)	0.04[c]
History of diabetes	34 (3.6)	588 (2.8)	0.13
History of hyperlipidemia	20 (2.1)	919 (4.3)	0.001[c]
History of heart comorbidities	10 (1.1)	165 (0.8)	0.34
History of stroke	7 (0.7)	59 (0.3)	0.01[c]
Current/ever smoker	234 (24.7)	5,153 (24.1)	0.71
Alcohol abuse	2 (0.2)	77 (0.4)	0.45[b]
Histology			0.25
WHO type 1	506 (53.3)	10,975 (51.4)	
WHO type 2	443 (46.7)	10,378 (48.6)	
T stage			0.03[c]
1–2	819 (86.3)	17,870 (83.7)	
3–4	130 (13.7)	3,483 (16.3)	
N stage			0.002[c]
0–1	564 (59.4)	15,539 (72.7)	
2	385 (40.6)	5,814 (27.2)	
AJCC stage group			0.006[c]
I–II	224 (23.6)	7,857 (36.8)	
III–IVa	725 (76.4)	13,496 (63.2)	
Concurrent chemotherapy	515 (54.3)	11,192 (52.4)	0.26
Radiotherapy method			<0.001[c]
CRT	741 (78.1)	10,739 (50.3)	
IMRT	208 (21.9)	10,614 (49.7)	

[a]The *P* value was calculated by χ^2 test, unless otherwise indicated by "[b]";
[b]The *P* value was calculated by Fisher exact test;
[c]Statistically significant.
P values were calculated to compare patients with and without RRNC.
CCI, Charlson Comorbidity Index; AJCC, American Joint Committee on Cancer.

previous publication (37–39). According to three rounds of confirmation by different Cox regression models, we conclude that advanced stage of NPC (HR = 2.22), greater total D_{max} (HR = 1.09), and reirradiation (HR = 1.10) were independent risk factors ($P < 0.001$ for all independent variables) for RIBI onset, while IMRT (compared with CRT) and hyperfractionation (compared to standard fractionation) were significantly correlated with lower risk of RIBI occurrence (**Table 2**).

Radiation-induced cranial nerve palsy

The median latency was 4.45 years, indicating it as the earliest-onset RRNC. Among the 597 cases, frequently impaired cranial nerves were vestibule-cochlear nerve [cranial nerve (CN) VIII, 228/597], posterior group of cranial nerves responsible for palatine movement (CN IX/X/XII, 219/597), group of cranial nerves responsible for eyeball movement (CN III/IV/VI, 50/597), and optic nerve (CNII, 45/597).

In adjusted multivariable Cox models, advanced stage of NPC (HR = 1.61, $P < 0.001$), CRT (HR = 1.68, $P < 0.001$), greater total Dmax of radiation (HR = 1.02, $P < 0.05$), and reirradiation (HR = 1.12, $P < 0.05$) were significantly associated with elevated risk of cranial nerve palsy onset (**Table 2**). In other words, patients still benefited from IMRT in terms of preventing damages to both the central nervous system and cranial nerves.

Specifically, CN VIII impairment tended to occur more frequently in post-CRT patients; While CN III/IV/VI were more likely to be impaired in post-IMRT ones (Supplementary Fig. S2).

Carotid artery stenosis

949 individuals received radiological examinations of bilateral carotid vessels, including ultrasonography, CTA, and MRA. 321 (1.44%) were diagnosed as carotid artery stenosis, including 17.4% (56/321) with significant stenosis and 83.6% (265/321) with mild to moderate stenosis. The median latency was 5.00 years.

Table 2. Treatment-related AEs reported in >2 patients treated with GEN1046 (n = 61).

		RIBI				Cranial nerve palsy				Carotid stenosis			
			Adjusted HR (95% CI)				Adjusted HR (95% CI)				Adjusted HR (95% CI)		
Variables		Events/ Patients	Model 1	Model 2	Model 3	Events/ patients	Model 1	Model 2	Model 3	Events/ patients	Model 1	Model 2	Model 3
AJCC stage	I/II	140/8,081		Ref		123/8,081		Ref		108/8,081		Ref	
	III/IVA&B	439/14,221	3.78 (2.51–5.69)	3.01 (2.01–4.48)	2.22 (1.49–3.31)	474/14,221	1.92 (1.77–2.11)	1.69 (1.57–1.83)	1.61 (1.51–1.73)	312/14,221	1.04 (1.03–1.05)	1.03 (1.02–1.04)	0.67 (0.53–1.03)
Concurrent chemotherapy	No	297/10,595		Ref		278/10,595		Ref		238/10,595		Ref	
	Yes	282/11,707	1.26 (1.06–1.50)	1.14 (0.96–1.34)	0.98 (0.83–1.15)	319/11,707	1.31 (1.12–1.54)	1.17 (1.00–1.37)	1.06 (0.91–1.24)	182/11,707	1.54 (1.26–1.88)	1.45 (1.20–1.76)	1.28 (1.05–1.57)
RT method	IMRT	148/11,480		Ref		112/11,480		Ref		108/11,480		Ref	
	CRT	431/10,822	3.09 (2.51–3.81)	2.45 (1.98–3.04)	2.11 (1.70–2.63)	485/10,822	2.70 (2.25–3.24)	1.90 (1.58–2.29)	1.68 (1.39–2.03)	312/10,822	2.47 (1.98–3.09)	1.73 (1.38–2.18)	1.57 (1.25–1.98)
Total D_{max}	Low	89/12,869		Ref		88/12,869		Ref		100/12,869		Ref	
	High	490/9,433	1.13 (1.12–1.15)	1.10 (1.01–1.03)	1.09 (1.08–1.11)	509/9,433	1.14 (1.12–1.15)	1.09 (1.07–1.10)	1.02 (1.01–1.03)	320/9,433	1.09 (1.08–1.11)	1.06 (1.04–1.07)	1.05 (1.04–1.07)
Fractionation	Hyper	120/5,514		Ref		73/5,514		Ref		48/5,514		Ref	
	Standard	459/16,210	1.98 (1.54–2.56)	1.86 (1.44–2.40)	1.35 (1.03–1.76)	524/16,210	1.90 (1.49–2.43)	1.39 (1.09–1.77)	1.12 (0.87–1.45)	372/16,210	1.84 (1.36–2.5)	1.37 (1.01–1.87)	1.21 (0.89–1.66)
Reirradiation	No	508/21,990		Ref		517/21,990		Ref		369/21,990		Ref	
	Yes	71/312	1.49 (1.24–1.99)	1.27 (1.13–1.54)	1.10 (1.02–1.48)	80/312	2.07 (1.05–3.09)	1.31 (1.10–2.17)	1.12 (1.09–1.17)	51/312	1.37 (1.09–2.14)	1.13 (1.10–1.19)	1.07 (1.05–1.10)

		Post-radiotherapy stroke				Hypopituitarism				Secondary epilepsy			
			Adjusted HR (95% CI)				Adjusted HR (95% CI)				Adjusted HR (95% CI)		
Variables		Events/ patients	Model 1	Model 2	Model 3	Events/ patients	Model 1	Model 2	Model 3	Events/ patients	Model 1	Model 2	Model 3
AJCC stage	I/II	36/8,081		Ref		28/8081		Ref		49/8,081		Ref	
	III/IVA&B	140/14,221	1.65 (1.44–1.96)	1.60 (1.41–1.89)	0.74 (0.50–1.10)	293/14,221	1.52 (1.36–1.76)	1.18 (0.85–1.65)	1.06 (0.94–1.27)	138/14,221	1.62 (1.46–2.63)	1.13 (1.02–1.47)	0.72 (0.46–1.29)
Concurrent chemotherapy	No	83/10,595		Ref		126/10,595		Ref		105/10,595		Ref	
	Yes	93/11,707	0.97 (0.69–1.38)	0.88 (0.63–1.24)	0.81 (0.57–1.15)	195/11,707	1.60 (1.20–2.17)	1.40 (1.05–1.88)	1.36 (1.01–1.83)	82/11,707	0.77 (0.56–1.05)	0.82 (0.60–1.14)	0.92 (0.66–1.27)
RT method	IMRT	31/11,480		Ref		72/11,480		Ref		44/11480		Ref	
	CRT	145/10,822	2.99 (1.94–4.62)	2.67 (1.72–4.12)	2.09 (1.68–2.60)	249/10,822	3.04 (2.11–4.37)	1.56 (1.06–2.29)	1.49 (1.07–2.06)	143/10,822	2.74 (1.95–3.85)	2.02 (1.43–2.87)	1.80 (1.26–2.57)
Total Dmax	Low	60/12,869		Ref		134/12,869		Ref		43/12,869		Ref	
	High	116/9,433	1.12 (1.08–1.15)	1.10 (1.07–1.13)	1.09 (1.06–1.13)	187/9,433	2.02 (1.17–3.49)	1.18 (1.14–1.21)	1.06 (1.03–1.09)	144/9,433	1.10 (1.07–1.12)	1.06 (1.03–1.08)	1.05 (1.03–1.08)
Fractionation	Hyper	18/5,514		Ref		31/5,514		Ref		19/5,514		Ref	
	Standard	158/16,210	1.38 (0.83–2.28)	1.10 (0.66–1.84)	0.80 (0.47–1.35)	290/16,210	2.37 (2.02–4.62)	1.82 (1.02–3.05)	1.44 (0.84–2.45)	168/16,210	2.52 (1.56–4.09)	1.90 (1.17–3.09)	1.70 (1.04–2.81)
Reirradiation	No	154/21,990		Ref		276/21,990		Ref		169/21,990		Ref	
	Yes	22/312	1.27 (1.13–1.51)	1.08 (1.04–1.16)	1.03 (0.49–2.48)	45/312	1.18 (0.85–1.65)	1.16 (0.83–1.62)	1.21 (0.86–1.69)	18/312	1.77 (1.08–2.92)	1.65 (1.01–2.67)	1.21 (0.66–2.22)

Note: Model 1 was adjusted for age, gender, and residency. Model 2 was additionally adjusted for lifestyle-related behaviors (smoking and excessive alcohol consumption) and comorbidities (hypertension, diabetes mellitus, hyperlipidemia, coronary heart disease, and prior stroke). Model 3 was additionally (compared with Model 2) adjusted for tumor- and treatment-related parameters other than the one being studied.

As indicated by **Table 2**, independent predictors of post-radiotherapy carotid stenosis were identified as concurrent chemotherapy (HR = 1.28, $P < 0.001$), CRT (HR = 1.57, $P < 0.001$), high-leveled total D_{max} (HR = 1.05, $P < 0.05$), and reirradiation to head and neck region (HR = 1.07, $P < 0.05$).

319 out of the 321 carotid stenosis cases were then followed more than once by carotid ultrasonography, while the other 3 out of 321 were lost to follow-up. Univariable analysis by χ^2 test showed significant stenosis was positively correlated with age at receiving ultrasound scanning ($P = 0.02$), comorbidity index ($P = 0.02$), and interval from radiotherapy ($P = 0.03$). They were further confirmed as independent predictors of significant carotid stenosis (**Table 3**). Thickening of IMT and narrowing of carotid lumen occurred predominantly in the first two years after radiotherapy, whereas the relative developing speed were not correlated with radiotherapy method (Supplementary Fig. S3).

Post-radiotherapy stroke

176 patients developed post-radiotherapy stroke (127 with ischemic stroke, 29 with hemorrhagic stroke and 20 with post-infarction hemorrhagic transformation or overlapping attack), with an incidence of 0.79%. Incidence was 0.57% (127/22,302) for ischemic stroke only, 0.13% (29/22,302) for hemorrhagic stroke only, and 0.09% (20/22,302) for dual attacks. Median latency was 5.25 years.

Positive associations with post-radiotherapy stroke were suggested for high-leveled total doses of radiation (HR = 1.09, $P < 0.05$). Conversely, a reduced risk (HR = 1.80 for CRT group, $P < 0.001$) was observed in patients with NPC receiving IMRT (**Table 2**).

Radiation-induced hypopituitarism

Hypopituitarism demonstrated an incidence of 0.72% (161/22,302), and the median latency was 5.00 years.

According to the results from the third Cox regression model shown in **Table 2**, IMRT and lower doses of radiation were both related to a lower risk of hypopituitarism morbidity (HR = 1.49, $P < 0.001$ in CRT cohort and HR = 1.06, $P < 0.05$ for higher D_{max} cohort). On the contrary, a higher hazard was independently correlated with concurrent chemotherapy (HR = 1.36, $P < 0.05$).

Secondary epilepsy

A total of 187 (0.84%) new events of epilepsy occurred during a median follow-up of 7.5 years (interquartile range, 4.1–11.0 years). Common forms included complex partial seizure (64/187) and generalized tonic-clonic seizure (62/187). Relatively rare forms included simple partial seizure (31/187), atonic seizure (20/187), and status epilepticus (10/187). Median latency was 5.10 years. Notably, there were 51 epilepsy patients (27.3%) with concurrent radiologically confirmed RIBI, while the remaining 136 were RIBI-free.

Results from multivariable Cox regression analysis (**Table 2**) indicated the risk of secondary epilepsy in CRT group was 1.80-fold higher (adjusted HR, Model 3, the same below) than that in CRT. 1.70-fold higher risk was identified in standard fractionation cohort, compared with hyperfractionated populations. Besides, risk increased as D_{max} increased (HR = 1.05, $P < 0.05$).

Dosimetric analysis

Due to the long time span as well as heterogeneity of institutions where patients received their initial radiotherapy, it is hard to collect complete dosimetric parameters from radiotherapy records of all patients enrolled. As can be seen in Supplementary Table S4, only 2252 complete radiotherapy records including D_{max} to OARs were found, in which 201 cases of RRNCs were identified. Considering the integrity of datasets, so far, we could only choose OARs located in central nervous system for further analysis. Averaged D_{max} to temporal

Table 3. Patient characteristics stratified based on radiotherapy method and level of carotid artery stenosis.

	No. (%)			No. (%)				
Variables	**CRT**	**IMRT**	***P* value[a]**	**Mild stenosis**	**Significant[b] stenosis**	***P* value[a]**	**HR (95% CI)**	***P* value[c]**
Age (y)								
≤54	123 (51.7)	36 (44.4)	0.26	115 (54.5)	44 (40.7)	0.02[d]	1.64 (1.07–3.07)	0.01[d]
>54	115 (48.3)	45 (55. 6)		96 (45.5)	64 (59.3)			
Gender								
Male	181 (76.1)	58 (71.6)	0.43	158 (74.9)	81 (75.0)	0.98	—	—
Female	57 (24.0)	23 (28.4)		53 (25.1)	27 (25.0)			
Smoking								
Current/ever	37 (15.6)	18 (22.2)	0.17	34 (16.1)	21 (19.4)	0.46	—	—
Never	201 (84.5)	63 (77.8)		177 (83.9)	87 (80.6)			
CCI								
=0	208 (87.4)	72 (88.9)	0.09	198 (93.8)	82 (75.9)	0.02[d]	1.63 (1.14–3.07)	0.01[d]
≥1	30 (12.6)	9 (11.1)		13 (6.2)	26 (24.1)			
RT method								
CRT	—	—	—	152 (72.0)	86 (79.6)	0.14	—	—
IMRT	—	—	—	86 (28.0)	22 (20.4)			
Latency (y)								
≤4	97 (40.8)	42 (51.9)	0.08	101 (47.9)	38 (35.2)	0.03[d]	1.61 (1.03–3.03)	0.02[d]
>4	141 (59.2)	39 (48.2)		110 (52.1)	70 (64.8)			

[a]*P* values were calculated by Pearson χ^2 test.
[b]According to the description of Steele and colleagues and Lam and colleagues, significant stenosis was defined as stenosis of >50% or occlusion.
[c]*P* values were calculated using multivariate Cox regression model.
[d]Statistically significant.

lobes, brainstem, and hypothalamus/pituitary gland are 72.43, 60.94, and 56.67 Gy, respectively. The Cox regression analysis in this cohort also revealed a significant correlation of RRNCs with D_{max} to OARs. Hence, higher D_{max} to the temporal lobes/brainstem/hypothalamus/pituitary gland served as a predictor for an increased risk of RRNCs.

Survival and cause-of-death analysis

There were 6,148 (27.6%) deaths recorded in the post-radiotherapy NPC cohort and 183 (19.3%) deaths in RRNC cohort during a median follow-up of 54.0 months (interquartile range, 30.0–216.0 months). Based on follow-up data from the 700 RRNC individuals with complete records and definitive outcomes, cumulative death rate was significantly lower in patients treated by IMRT compared with CRT ($P = 0.03$, **Fig. 1A**). Constituent ratios for causes of death in RRNC and RRNC-free groups were different (**Fig. 2**). Cardinal cause of death in RRNC patients was severe pneumonia ($N = 78$, 42.2%), while massive NPC bleeding with concurrent hypovolemic shock became the major cause of death in RRNC-free patients. As shown in **Fig. 3**, severe pneumonia,

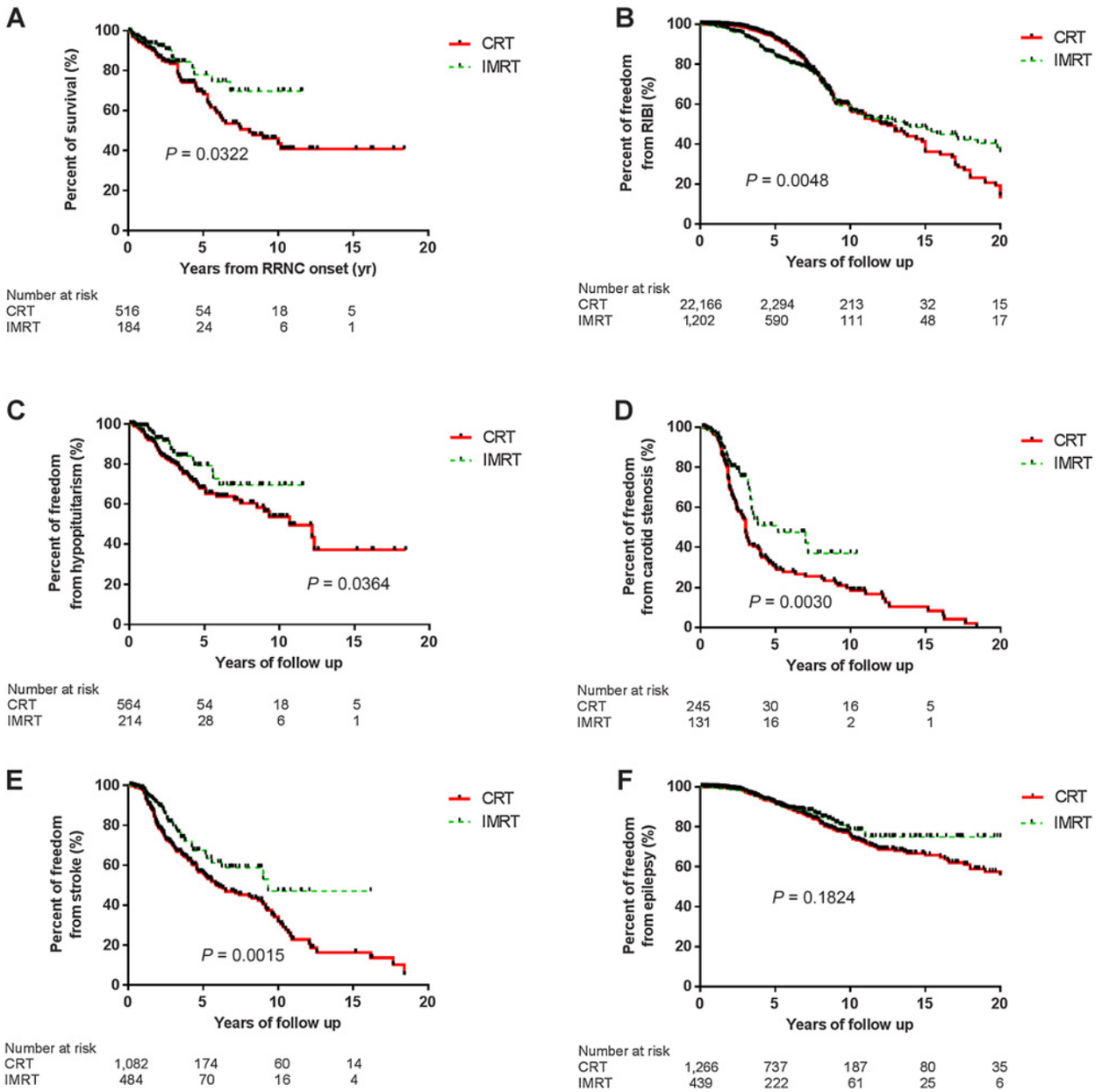

Figure 1.

Kaplan-Meier curves indicating mortality and RRNCs-free survival over time by method groups: **A,** (RRNC cohort) crude mortality. **B,** (post-radiotherapy NPC cohort) RIBI-free survival. **C,** Hypopituitarism-free survival. **D,** Carotid stenosis-free survival. **E,** Stroke-free survival. **F,** Epilepsy-free survival.

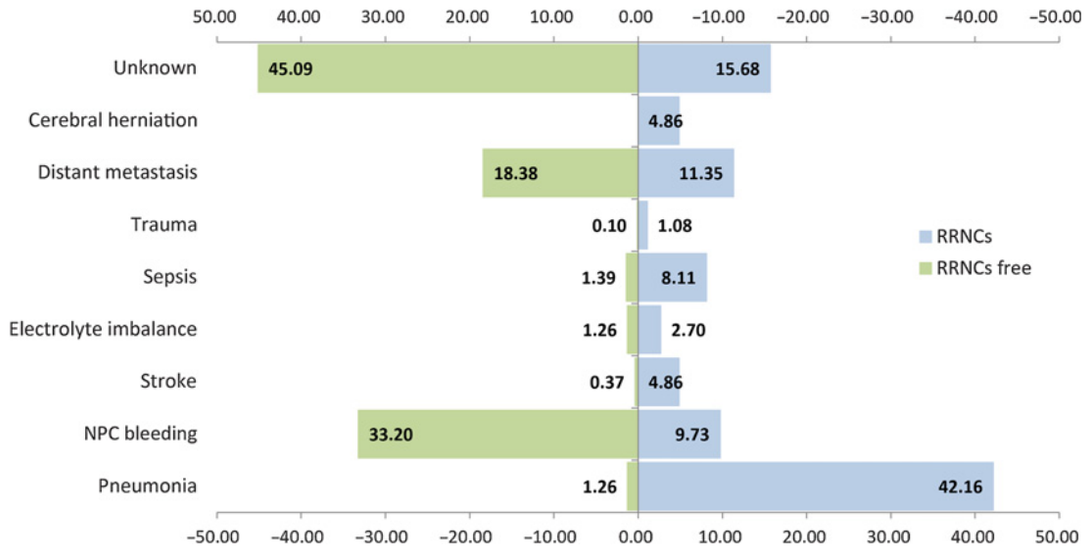

Figure 2.
Grouped bar graph illustrating proportionally different causes of death in RRNC and RRNC-free subgroup of patients with post-radiotherapy NPC.

life-threatening stroke, severe electrolyte imbalance, and sepsis were significant covariates contributing to different death rate between these two groups of patients.

Log-rank tests suggested there was a significant difference in RIBI-free survival between post-CRT patients and post-IMRT ones ($P = 0.005$, **Fig. 1B**). Likewise, IMRT demonstrated significant complication-free survival advantages over CRT, including hypopituitarism, carotid stenosis, and stroke (either ischemic or hemorrhagic; **Fig. 1C–E**). No significant epilepsy-free (**Fig. 1F**) benefit of IMRT over CRT was observed.

Discussion

Different from previous studies on RRNCs, which mainly focused on single disease category among the spectrum, our research provides a widening view both in central nervous system and peripheral nervous system, covers most neurologic complications, and illustrates this spectrum of diseases in a more comprehensive way.

During the pre-IMRT era, CRT, especially 3D-CRT, was successfully used to treat NPC as an alternative as well as a boosting technique to 2D-RT (40). Soon after the clinical application of IMRT in the treatment of NPC, the short-term results of IMRT suggested improved survival outcomes and quality of life (41). Recent comparative clinical studies, both prospective and retrospective, have compared the advantages of IMRT over 2D-RT or 3D-CRT (35–36, 42). An improved dosage coverage of advanced primary T3–4 tumors by IMRT led to better local control than 2D-CRT in recent clinical settings, which greatly facilitates the widening applications of IMRT over CRT nowadays (35). These findings were consistent with ours, proving that IMRT served as an independent protective factor for all kinds of RRNCs.

The overall incidence of RRNC here is higher than previously reported (15, 43–45), partially explained by administration of higher-resolution radiologic equipment (46, 41, 42) with more comprehensive and sensitive detection for minor lesions even before the onset of symptoms. However, relatively lower rates of CN injury and temporal lobe epilepsy (26, 35) could be attributed to exclusion of radiotherapy-irrelevant conditions (e.g., individuals with NPC recurring and involving into nearby cranial nerves) and missed diagnosis of temporal lobe epilepsy solely with olfactory hallucination. In addition, there are inevitably confounding effects brought by some unmeasured variables (e.g., socioeconomic status, penetration rate of advanced IMRT/3D-CRT techniques, and utilization of MRI for RIBI detection) and preexisted heterogeneity across the enrolled regions [populational prevalence of current smoking in Guangdong, Guangxi, and Hainan from 2003 to 2013 was >25%, 20%–25%, and <20%, respectively (47)]. This is one of the major contributors to the differences in risk for each RRNC by province (**Table 2**). Moreover, radiotherapy-related neuropathic pain was the only component worse with IMRT than CRT. Cryptogenic neuropathic pain makes it difficult to diagnose. More delicate parameters regarding radiotherapy process, like dose-volume histogram (DVH), planning target volume (PTV), and dose fractionation among OARs, are needed in more specific clinical trials to clarify the phenomenon.

Conversely, our results indicate that patients receiving IMRT are at higher risk of cranial nerve palsy involving vision pathway, eyeball movement and posterior group, with statistical or marginally statistical significance. Direct comparison of cranial nerve injuries between CRT and IMRT is not enough if the indication of these technologies depends on the anatomical distribution of the primary and nodal diseases. Dose to the OARs is controlled in IMRT and the prescribed dose to the OARs can be totally different between these two techniques. It is most likely that the radiotherapy team has selected IMRT rather than CRT for the patients with tumors which involve into cranial nerves responsible for vision conduction, eyeball movement and swallowing, since most initially diagnosed NPC patients tend to present as cranial nerve palsy with blurred or doubled vision, eyeball fixation, and dysphagia. On the premise, the complication rate in cranial nerve involvement must be higher in IMRT since dose for cranial nerve in CRT is not required to be that high.

There are several limitations of our study. First, some essential details of radiotherapy that may potentially contribute to RRNCs

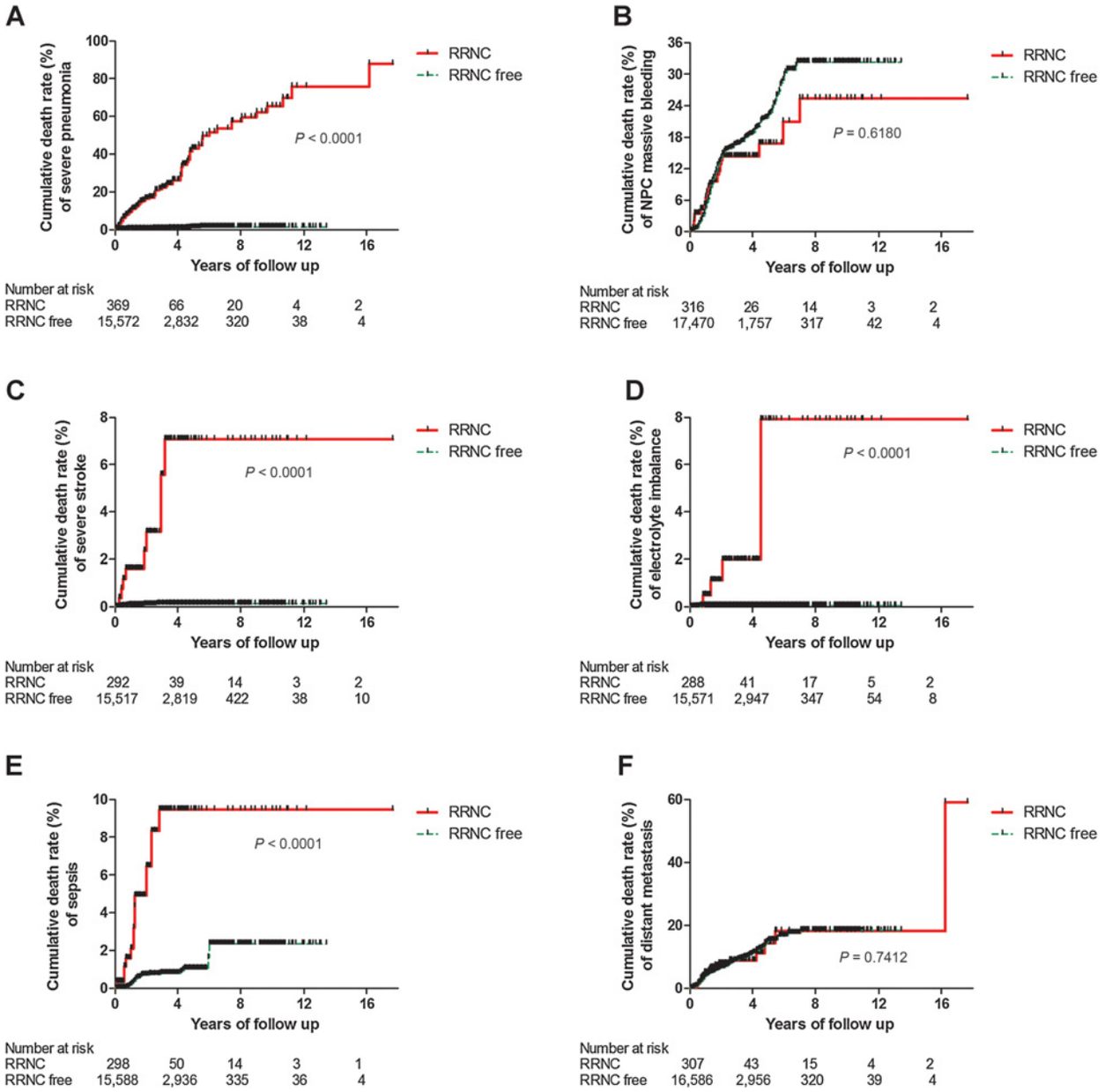

Figure 3.

Kaplan–Meier curves indicating cumulative event rate by specific causes of deaths in RRNC versus RRNC-free cohort: **A**, severe aspiration pneumonia; **B**, NPC massive bleeding; **C**, life-threatening stroke; **D**, severe electrolyte imbalance; **E**, sepsis; **F**, distant metastasis-induced cachexia.

development were not addressed due to lack of complete radiotherapy records in such a large cohort, including dose-volume curves, field arrangement, and planning risk volumes (PRV). Second, our conclusions were developed from a cohort of patients from NPC endemic areas in Southern China, and generalizability to patients from different regions and ethnicities may deserve further confirmation. Furthermore, our datasets were obtained retrospectively, and some important outcome parameters, like grading of disease severity and quality-of-life scores, were not accurate enough due to lack of a consistent measurement standard. Prospective studies with well-designed protocols and sufficient sample size are awaited to validate our findings.

Authors' Disclosures

No disclosures were reported.

Authors' Contributions

T. Pan: Conceptualization, data curation, software, formal analysis, methodology, writing–original draft, project administration. **X. Li:** Data curation, formal analysis, supervision, methodology, writing–original draft, project administration.

B. Zhao: Conceptualization, data curation, formal analysis, supervision, methodology, writing–original draft. **C. Zhang:** Conceptualization, data curation, formal analysis, writing–original draft, project administration. **X. Rong:** Software, formal analysis, supervision, writing–original draft, writing–review and editing. **C. Qin:** Resources, data curation, formal analysis, project administration. **G. Wen:** Resources, data curation, formal analysis. **W. Wu:** Resources, data curation. **H. Wang:** Software, formal analysis, writing–review and editing. **K. Lu:** Resources, data curation. **H. Zhou:** Resources, data curation. **Y. Peng:** Conceptualization, resources, supervision, funding acquisition, methodology, project administration, writing–review and editing.

Acknowledgments

This project was supported by Grant 81572481 (to Y. Peng) from National Natural Science Foundation of China. We sincerely thank Dr. Wen Chen (Department of Medical Statistics and Epidemiology, School of Public Health, Sun Yat-Sen University) for help and support during early planning especially in statistical consulting. We sincerely thank Professor Yimin Liu (Department of Radiation Oncology, Sun Yat-Sen Memorial Hospital, Sun Yat-Sen University) for supervising clinical data concerning radiotherapy parameters and regimen. The authors assume full responsibility for analyses and interpretation of these data.

The costs of publication of this article were defrayed in part by the payment of page charges. This article must therefore be hereby marked *advertisement* in accordance with 18 U.S.C. Section 1734 solely to indicate this fact.

Received August 9, 2021; revised October 16, 2021; accepted February 21, 2022; published first February 24, 2022.

References

1. Lee AW, Ng SH, Ho JH, Tse VK, Poon YF, Tse CC, et al. Clinical diagnosis of late temporal lobe necrosis following radiation therapy for nasopharyngeal carcinoma. Cancer 1988;61:1535–42.
2. Bray F, Ferlay J, Soerjomataram I, Siegel RL, Torre LA, Jemal A. Global cancer statistics 2018: GLOBOCAN estimates of incidence and mortality worldwide for 36 cancers in 185 countries. CA Cancer J Clin 2018;68:394–424.
3. Wei KR, Zheng RS, Zhang SW, Liang ZH, Li ZM, Chen WQ. Nasopharyngeal carcinoma incidence and mortality in China, 2013. Chin J Cancer 2017;36:90.
4. Wei W, Zeng H, Zheng R, Zhang S, An L, Chen R, et al. Cancer registration in China and its role in cancer prevention and control. Lancet Oncol 2020;21: e342–9.
5. Chen YP, Chan ATC, Le QT, Blanchard P, Sun Y, MJ. Nasopharyngeal carcinoma. Lancet 2019;394:64–80.
6. Li WF, Sun Y, Chen M, Tang LL, Liu LZ, Mao YP, et al. Locoregional extension patterns of nasopharyngeal carcinoma and suggestions for clinical target volume delineation. Chin J Cancer 2012;31:579–87.
7. Chan YL, Leung SF, King AD, Choi PH, Metreweli C. Late radiation injury to the temporal lobes: morphologic evaluation at MR imaging. Radiology 1999;213: 800–7.
8. Zhou X, Ou X, Xu T, Wang X, Shen C, Ding J, et al. Effect of dosimetric factors on occurrence and volume of temporal lobe necrosis following intensity modulated radiation therapy for nasopharyngeal carcinoma: a case-control study. Int J Radiat Oncol Biol Phys 2014;90:261–9.
9. Miura M, Nakajima M, Fujimoto A, Kaku Y, Kawano T, Watanabe M, et al. High prevalence of small vessel disease long after cranial irradiation. J Clin Neurosci 2017;46:129–35.
10. Kong F, Zhou J, Du C, He X, Kong L, Hu C, et al. Long-term survival and late complications of intensity-modulated radiotherapy for recurrent nasopharyngeal carcinoma. BMC Cancer 2018;18:1139.
11. Lohia S, Rajapurkar M, Nguyen SA, Sharma AK, Gillespie MB, Day TA. A comparison of outcomes using intensity-modulated radiation therapy and 3-dimensional conformal radiation therapy in treatment of oropharyngeal cancer. JAMA Otolaryngol Head Neck Surg 2014;140:331–7.
12. Du QH, Gan YX, Wang RS, Liu WQ, Li J, Liang FF, et al. Half-brain delineation for prediction of radiation-induced temporal lobe injury in nasopharyngeal carcinoma receiving intensity-modulated radiotherapy. Front Oncol 2021;11: 599942.
13. Wei J, Shen Z, Wang H, Zhao Q, Ji R, Wang B, et al. Research progress on mechanism and dosimetry of brainstem injury induced by intensity-modulated radiotherapy, proton therapy, and heavy ion radiotherapy. Eur Radiol 2020;30: 5011–20.
14. Wang TM, Shen GP, Chen MY, Zhang JB, Sun Y, He J, et al. Genome-wide association study of susceptibility loci for radiation-induced brain injury. J Natl Cancer Inst 2019;111:620–8.
15. Yao CY, Zhou GR, Wang LJ, Xu JH, Ye JJ, Zhang LF, et al. A retrospective dosimetry study of intensity-modulated radiotherapy for nasopharyngeal carcinoma: radiation-induced brainstem injury and dose-volume analysis. Radiat Oncol 2018;13:194.
16. Tang LL, Chen YP, Mao YP, Wang ZX, Guo R, Chen L, et al. Validation of the 8th edition of the UICC/AJCC staging system for nasopharyngeal carcinoma from endemic areas in the intensity-modulated radiotherapy era. J Natl Compr Canc Netw 2017;15:913–5.
17. Smith GL, Smith BD, Buchholz TA, Giordano SH, Garden AS, Woodward WA, et al. Cerebrovascular disease risk in older head and neck cancer patients after radiotherapy. J Clin Oncol 2008;26:5119–25.
18. Koppelmans V, Vernooij MW, Boogerd W, Seynaeve C, Ikram MA, Breteler MM, et al. Prevalence of cerebral small-vessel disease in long-term breast cancer survivors exposed to both adjuvant radiotherapy and chemotherapy. J Clin Oncol 2015;33:588–93.
19. Zhao S, Zhou T, Ma S, Zhao Y, Zhan J, Fang W, et al. Effects of thoracic radiotherapy timing and duration on progression-free survival in limited-stage small cell lung cancer. Cancer Med 2018;7:4208–16.
20. Zeng L, Huang SM, Tian YM, Sun XM, Han F, Lu TX, et al. Normal tissue complication probability model for radiation-induced temporal lobe injury after intensity-modulated radiation therapy for nasopharyngeal carcinoma. Radiology 2015;276:243–9.
21. Xu L, Yao JJ, Zhou GQ, Zhang WJ, Liu GL, Liu LZ, et al. The impact of clinical stage on radiation doses to organs at risk following intensity-modulated radiotherapy in nasopharyngeal carcinoma: A prospective analysis. J Cancer 2016;7: 2157–64.
22. Suresh K, Voong KR, Shankar B, Forde PM, Ettinger DS, Marrone KA, et al. Pneumonitis in non–small cell lung cancer patients receiving immune checkpoint immunotherapy: Incidence and risk factors. J Thorac Oncol 2018;13:1930–9.
23. Mao YP, Zhou GQ, Liu LZ, Guo R, Sun Y, Li L, et al. Comparison of radiological and clinical features of temporal lobe necrosis in nasopharyngeal carcinoma patients treated with 2D radiotherapy or intensity-modulated radiotherapy. Brit J Cancer 2014;110:2633–9.
24. Kumar AJ, Leeds NE, Fuller GN, Van Tassel P, Maor MH, Sawaya RE, et al. Malignant gliomas: MR imaging spectrum of radiation therapy- and chemotherapy-induced necrosis of the brain after treatment. Radiology 2000; 217:377–84.
25. Wang YX, King AD, Zhou H, Leung SF, Abrigo J, Chan YL, et al. Evolution of radiation-induced brain injury: MR imaging-based study. Radiology 2010;254: 210–8.
26. Luk YS, Shum JS, Sze HC, Chan LL, Ng WT, Lee AW. Predictive factors and radiological features of radiation-induced cranial nerve palsy in patients with nasopharyngeal carcinoma following radical radiotherapy. Oral Oncol 2013;49: 49–54.
27. Huang CC, Fang FM, Chen HC, Hsu HC, Huang TL, Su YL, et al. Therapeutic outcome of nasopharyngeal carcinoma with cranial nerve palsy: a single institution experience of 104 patients. Onco Targets Ther 2017;4:2069–75.
28. Zhou L, Xing P, Chen Y, Xu X, Shen J, Lu X. Carotid and vertebral artery stenosis evaluated by contrast-enhanced MR angiography in nasopharyngeal carcinoma patients after radiotherapy: a prospective cohort study. Br J Radiol 2015;88:150–75.
29. Liao W, Zhou H, Fan S, Zheng Y, Zhang B, Zhao Z, et al. Comparison of significant carotid stenosis for nasopharyngeal carcinoma between intensity-modulated radiotherapy and conventional two-dimensional radiotherapy. Sci Rep 2018;8:138–99.
30. Chu CN, Chen PC, Bai LY, Muo CH, Sung FC, Chen SW. Young nasopharyngeal cancer patients with radiotherapy and chemotherapy are most prone to ischaemic risk of stroke: a national database, controlled cohort study. Clin Otolaryngol 2013;38:39–47.

31. Ipekci SH, Cakir M, Kiyici A, Koc O, Artac M. Radiotherapy-induced hypopituitarism in nasopharyngeal carcinoma: the tip of an iceberg. Exp Clin Endocrinol Diabete 2015;123:411–8.
32. Liao H, Zhu Z, Rong X, Wang H, Peng Y. Hyponatremia is a potential predictor of progression in radiation-induced brain necrosis: a retrospective study. BMC Neurol 2018;18:130–1.
33. Kong C, Zhu XZ, Lee TF, Feng PB, Xu JH, Qian PD, et al. LASSO-based NTCP model for radiation-induced temporal lobe injury developing after intensity-modulated radiotherapy of nasopharyngeal carcinoma. Sci Rep 2016;6:263–78.
34. Korff CM, Scheffer IE. Epilepsy classification: a cycle of evolution and revolution. Curr Opin Neurol 2013;26:163–7.
35. Rong X, Yin J, Wang H, Zhang X, Peng Y. Statin treatment may lower the risk of postradiation epilepsy in patients with nasopharyngeal carcinoma. Epilepsia 2017;58:2172–7.
36. Jiang J, Li Y, Shen Q, Rong X, Huang X, Li H, et al. Effect of pregabalin on radiotherapy-related neuropathic pain in patients with head and neck cancer: A randomized controlled trial. J Clin Oncol 2019;37:135–43.
37. Mayo C, Yorke E, Merchant TE. Radiation associated brainstem injury. Int J Radiat Oncol Biol Phys 2010;76:S36–41.
38. Gentile MS, Yeap BY, Paganetti H, Goebel CP, Gaudet DE, Gallotto SL, et al. Brainstem injury in pediatric patients with posterior fossa tumors treated with proton beam therapy and associated dosimetric factors. Int J Radiat Oncol Biol Phys 2018;100:719–29.
39. Milano MT, Grimm J, Niemierko A, Soltys SG, Moiseenko V, Redmond KJ, et al. Single- and multifraction stereotactic radiosurgery dose/volume tolerances of the brain. Int J Radiat Oncol Biol Phys 2021;110:68–86.
40. Wang S, Qiu D, So KF, Wu EX, Leung LH, Gu J, et al. Radiation induced brain injury: assessment of white matter tracts in a pre-clinical animal model using diffusion tensor MR imaging. J Neurooncol 2013;112:9–15.
41. Ng WT, Ngan RKC, Kwong DLW, Tung SY, Yuen KT, Kam MKM, et al. Prospective, multicenter, phase 2 trial of induction chemotherapy followed by bio-chemo-radiotherapy for locally advanced recurrent nasopharyngeal carcinoma. Int J Radiat Oncol Biol Phys 2018;100:630–8.
42. Yao JJ, Chen FP, Zhou GQ, Zhang WJ, Xu L, Wang XJ, et al. A prospective study on radiation doses to organs at risk (OARs) during intensity-modulated radiotherapy for nasopharyngeal carcinoma patients. Oncotarget 2016;7:21742–52.
43. Zhang LL, Zhou GQ, Li YC, Lin AH, Ma J, Qi ZY, et al. Induction chemotherapy has no prognostic value in patients with locoregionally advanced nasopharyngeal carcinoma and chronic hepatitis B infection in the IMRT era. Transl Oncol 2017;10:800–5.
44. Lin HC, Friedman M, Chang HW, Fang FM, Lin MC, Su MC. Impact of head and neck radiotherapy for patients with nasopharyngeal carcinoma on sleep-related breathing disorders. JAMA Otolaryngol Head Neck Surg 2014;140:1166–72.
45. Li YZ, Cai PQ, Xie CM, Huang ZL, Zhang GY, Wu YP, et al. Nasopharyngeal cancer: Impact of skull base invasion on patients' prognosis and its potential implications on TNM staging. Eur J Radiol 2013;82:e107–11.
46. Chen SC, Abe Y, Fang PT, Hsieh YJ, Yang YI, Lu TY, et al. Prognosis of hippocampal function after sub-lethal irradiation brain injury in patients with nasopharyngeal carcinoma. Sci Rep 2017;7:146–97.
47. Wang M, Luo X, Xu S, Liu W, Ding F, Zhang X, et al. Trends in smoking prevalence and implication for chronic diseases in China: serial national cross-sectional surveys from 2003 to 2013. Lancet Respir Med 2019;7:35–45.